

Lawrence Berkeley National Laboratory

Lawrence Berkeley National Laboratory

Title

A SOLAR TEST COLLECTOR FOR EVALUATION OF BOTH SELECTIVE AND NON-SELECTIVE ABSORBERS

Permalink

<https://escholarship.org/uc/item/4dc599mq>

Author

Lampert, Carl M.

Publication Date

1978-06-01

Submitted to the International
Journal of Solar Energy

LBL-6974
Preprint

RECEIVED
LAWRENCE
BERKELEY LABORATORY

C.2

AUG 30 1978

LIBRARY AND
DOCUMENTS SECTION

A SOLAR TEST COLLECTOR FOR EVALUATION OF BOTH
SELECTIVE AND NON-SELECTIVE ABSORBERS

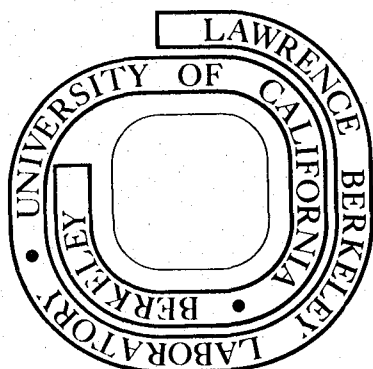
Carl M. Lampert and Jack Washburn

June 1978

Prepared for the U. S. Department of Energy
under Contract W-7405-ENG-48

TWO-WEEK LOAN COPY

This is a Library Circulating Copy
which may be borrowed for two weeks.
For a personal retention copy, call
Tech. Info. Division, Ext. 6782



LBL-6974

C.2

— LEGAL NOTICE —

This report was prepared as an account of work sponsored by the United States Government. Neither the United States nor the Department of Energy, nor any of their employees, nor any of their contractors, subcontractors, or their employees, makes any warranty, express or implied, or assumes any legal liability or responsibility for the accuracy, completeness or usefulness of any information, apparatus, product or process disclosed, or represents that its use would not infringe privately owned rights.

-iii-

A SOLAR TEST COLLECTOR FOR EVALUATION OF BOTH SELECTIVE AND
NON-SELECTIVE ABSORBERS

Carl M. Lampert and Jack Washburn

Materials and Molecular Research Division,
Lawrence Berkeley Laboratory
and

Department of Materials Science and Mineral Engineering,
College of Engineering; University of California
Berkeley, California 94720

ABSTRACT

A solar test collector was designed for the testing of thermally absorbing coatings under controlled conditions. The design consisted of a collector fed by a controlled temperature fluid within the range of 25-90°C (77-194°F). This temperature was maintained by a custom electronic controller. A small variable flow pump circulated water through three collector pipes at selected flow rates. Strip heaters coupled with a differential temperature controller compensated for edge losses associated with small collectors. Detailed design and operation data were presented and three black chrome and one non-selective absorber were analyzed in detail by test collector measurements. Results showed Efficiencies as high as 77% and 75% ($\Delta T = 0$) were obtained respectively for 1.0 μm black chrome on copper and nickel plated steel. The lowest loss coefficients were about 3.8 W/m²°C for all black chrome/metal surfaces with the highest being 8.4 W/m²°C for the black paint/metal sample. Also, a collector model was presented for comparison.

INTRODUCTION

A solar test collector was built to test different varieties of selective and non-selective surfaces, particularly black chrome, under realistic, repeatable, controlled and well recorded conditions. In this study the collector was used to compare different types of black chrome (Chromonyx), supplied by Harshaw Chemical Co., and a black painted surface. These surfaces are representative of both selective and non-selective coatings and optical values of these coatings can be correlated to test collector data. Selectivity is produced by optical properties which vary greatly from one spectral region to another. A solar selective surface efficiently captures the sun's energy in the high intensity visible and near infrared spectral regions, while exhibiting poor infrared radiating properties. Accordingly, a selective surface will absorb and retain a high amount of energy from the sun while a non-selective surface will lose most of its absorbed energy by radiation. The design and results of such described surfaces will be presented in the following sections.

EXPERIMENTAL APPARATUS AND PROCEDURES

Concept of Design

A solar test collector was designed so that certain collector parameters could be held constant or controlled and yet different coatings could be tested. this design allows different types of selective and non-selective surfaces to be tested and evaluated in terms of collection efficiency under various operating temperatures and flow rates. Results for various Chromonyx coatings will be presented later and compared with those for a black painted surface.

The main components of the collector consist of a body and cover, which houses three absorber pipes; a controlled temperature water bath; and a variable-flow pump.

The collector body is designed to permit easy removal of collector pipes. The body can be set any desired tilt angle with respect to the sun, to suit the season of the year. The collector pipes consist of a metallic material (e.g., copper or steel), although not a stringent requirement, coated with a selective or non-selective surface. Of the three parallel pipes, the center pipe is the critically controlled and monitored one. The purpose of the two outside pipes is to restrict the amount of heat lost from the sides of the central pipe. Furthermore, controlled temperature heating stripes are placed under the two outside pipes to reduce overall edge losses. In this fashion, a small collector can simulate large collector surroundings along the central pipe. This simulation is achieved by a differential temperature controller which maintains constant temperatures at all pipe outlets by turning on strip heaters when required. Across the central pipe both inlet

and outlet temperatures are recorded with better than one degree ($^{\circ}\text{C}$) accuracy.

The collector is fed by a controlled temperature bath which supplies a fluid at a set, adjustable temperature in the range $25\text{-}90^{\circ}\text{C}$. This temperature is maintained by a custom electronic controller. A small variable-flow pump circulates water through three collector pipes according to a specified but adjustable flow rate. The fluid from the collector is passed into a cooling bath and is recirculated to the controlled temperature water bath. Simultaneous measurements are made of solar radiation, ambient temperature, wind direction and velocity. The flow chart for the collector, showing the significant features described, is depicted in Fig. 1. Photographs of complete test apparatus are shown in Figs. 2 and 3.

Collector Body Design

Collector Housing

The collector body consists of a wooden housing filled with shaped and molded insulation in which all collector test pipes are mounted along with valve systems and flowmeter. The collector is covered by a removable vapor proof double-glass cover. The insulation is Upjohn type Trymer CPR 9545 isocyanurate rigid cellular polyurethane foam. The completed housing is finished by two coats of durable enamel paint. Dow Corning silicone RTV adhesive sealant is used as caulking material.

Cover System

The wooden collector cover, consisting of two rectangular glass windows (ASG brand, low iron type) surrounded by a wooden frame and glazed with RTV sealant, provides a secure vapor proof protective

covering for the collector pipes. The purpose of the collector cover is to reduce the amount of heat loss from the pipes due to thermal convection. Also, the cover is important for suppression of radiation emitted by the absorber surface. The glass windows serve as a barrier for the infrared energy emitted by the absorber, thus acting to trap locally this thermal energy.

Incorporated into the collector cover system is a vapor barrier created by a flexible closed cell polyurethane high density spline. Where the cover passes over the three collector pipes a molded gasket attached to a removable wooden plate serves as a seal between the cover and body. The interconnection between the collector and cover can be viewed in Fig. 4.

Piping System

The piping which feeds and discharges fluid to the three collector pipes is insulated by polyurethane flexible foam. Fiberglass wool serves as an insulating medium between the flexible polyurethane foam and the rigid foam of the collector body. Strip heaters are placed between the foam insulation and bottom surfaces of the outer collector. These strip heaters are attached to strips of asbestos cloth by RTV silicone adhesive and then fastened to the polyurethane foam. Neoprene adhesive is also used to cover the exposed surfaces of the foam insulation to retard abrasion and weathering. The strip heaters are waterproof Briskeat type BS-41 which operate at 15 VAC and 192 Watts. These heaters are cycled on and off independently by a differential temperature controller. The placement of the two strip heaters can be viewed in Fig. 5.

The collector pipes may be any type material as long as they conform to approximately 3.8-4.2 cm outside diameter and 1.37 m long. The comparison of identical coatings on different substrate (pipe) materials is complicated by differences of thermal conductivity. Examples of different types of pipe materials are mild steel, copper, galvanized steel and aluminum. Also, a flat plate conforming to size specifications and inlet/outlet clearances could be tested in a similar manner as individual pipes. The position of the collector pipes can be seen in Figs. 4 and 5.

Flowmeters

The flowmeter system is designed to permit balanced and regulated flow of fluid through the three collector pipes. The fluid flow through the outer collector pipe is regulated by two matched needle valves. The flow in the center test pipe is monitored and controlled by a low-flow flowmeter/needle valve combination. This flowmeter is a Brooks Model 1515 custom made for 0-49 L/hr of water. The accuracy of this type of flowmeter is important due to its bearing upon the final calculation of collector efficiency.

Collector Pipe Coupling

The mating of a rigid brass pipe manifold with three threadless collector pipes initially presented a problem. This connection design also had to incorporate a thermocouple probe and was to be leakproof, compact, and easy to assemble on site.

The final design of the connector consists of a threaded brass tube which passes through the length of a rubber tapered plug. A nut, washer, and O-ring assembly holds the internal end tight while

a union fitting, washer and O-ring assembly provides the outer coupling. A thermocouple probe (Cal-Alloy brand copper-constantan ungrounded junction with a stainless steel sheath) is inserted through the rubber plug. Sealing of the collector pipes is achieved by tightening the union fitting against the rubber plug causing outward expansion of the plug by axial compression. A cross-sectional view of this connector plug and thermocouple is shown in Fig. 6. Also, note that the collector pipes are slightly beveled inside to remove burrs.

Test Collector Tilting Stand

To orient the collector a stand is needed which has the ability to tilt the collector so it will be perpendicular to the sun's rays at solar noon. The stand is designed for an overall range of $12-62^{\circ}$ tilt angle (with respect to horizontal plane) adjustable in 1° increments. The collector stand is designed for 37.8° north latitude (Berkeley area) where the optimum tilt varies from $12-62^{\circ}$. The collector tilting stand may be viewed in Figs. 2 and 3 supporting the test collector.

Pumping, Heating and Storage Supplies

Pumping System Design

For pumping of collector fluid a Flotec brand electric self priming pump, Model R2B1-1100 v is used. It is equipped with a variable displacement cone which can be adjusted at an angle in such a way that the flow through the pump varies. The adjustment of cone angle is simple and can be done while the pump is in operation. In conjunction with a feedback piping system a large range of pumping flow rates can be achieved, 0-22 L/min. A Blue White Industries, Model F-400, primary flowmeter is used to monitor the total fluid flow into the

collector body. the flowmeter has a range from 0-227 L/hr. The initial flows in all three collector pipes are set by use of the primary flowmeter in combination with feedback valve and cone adjustments. The flows can be balanced amongst the three pipes by needle valves in conjunction with the central pipe flowmeter. The arrangement of flowmeter and feedback system is represented in Fig. 1.

Heater and Storage System Design

An electric water heater serves both as a source for supplying temperature controlled water and storage tank for hot water. The water heater is a Sears, Roebuck and Co. fast recovery model No. 183.32123. This water heater has a 20 gal capacity with a 1650 watt, 120 VAC heating element. The stock thermostat has been bypassed and heating is controlled by a 20 ampere mercury relay which is actuated by a solid state temperature controller. An auxiliary storage tank is used to buffer and to cool down hot collector effluent. This 18 gal tank can be disconnected from the system by two manual control valves. The auxiliary tank is necessary for cooling when the collector's effluent temperature ranges from 65 to 99°C, typical of low flow rates. The tank arrangement can be viewed best in Fig. 2.

Collector Electronic Controller

Controller Design Constraints

The control system was designed to perform three basic functions. First, it must be able to regulate accurately the fluid inlet temperature to the collector, while being able to allow for an adjustable range of temperatures, chosen by the operator (up to 100°C). Also, the system must be able to sense different pipe outlet temperatures and

cycle on strip heaters to the outer pipes when their temperatures are lower than the central pipe. The final function is that the system must provide linear output signals, which indicate the various collector temperatures, in such a way that they may be fed easily into a recording device. Also, the controller must be resistant to the consequences of a difficult operating environment. A chief problem is power line transients bypassing the power supply and falsely triggering the control instrumentation. Since the controller circuitry senses microvolt changes at its input stages, noise or spikes on the order of volts originating from the power line can easily find their way into the signal circuitry, causing false readings. The circuitry was designed to handle such random interruptions.

Another consideration is to restrict the range of the operating temperatures of the entire electronic assembly. If there is a large variation in temperature, electronic circuitry calibration will be unstable.

Fortunately, very little heat is self-generated when using solid state circuitry. The major problem is the magnitude change of the ambient temperature of the rooftop environment. This problem was solved by proper shielding and temperature calibration of the control circuits.

Controller System

The controller makes decisions and operates various heaters to compensate for outer collector pipe losses, and to regulate inlet water temperature.

The strip heater control system obtains its signals from the collector pipe outlet thermocouples. The outer pipe signals are compared to that of the central test pipe. Depending upon the difference in signals the heaters will turn on or off independently.

Another circuit controls the water heater element. In this case the thermocouple signal is obtained at the inlet of the central pipe. This signal is compared to a set, adjustable voltage, calibrated in degrees. When the inlet temperature is lower than the set temperature, the water heater will operate. When the inlet temperature appears the same or greater (probably it will never greater than the set temperature) the heater will be off. The complete control diagram is depicted in Fig. 7.

Shown in Fig. 7 are also many significant technical details. The inputs of the four channels pass through two amplifier stages. The first stage is for basic filtering and smoothing with an amplification gain of 100; the second stage contains a low pass filter and further amplification of 25. The second amplifier also acts as a summing amplifier for the temperature compensation and offset signals. The overall gain of both stages is 2500 with an output of 100 millivolts per degree celsius. Another operational amplifier is used to filter and boost the reference junction voltage from the temperature compensation unit. Temperature compensation is achieved by use of a diode signal (exhibiting a linear temperature dependence with voltage) which is calibrated and amplified to simulate an ice point reference (0°C), with respect to ambient temperature. Also necessary to such a design is to have the input thermocouples referenced initially to

the ambient temperature. This requirement is satisfied by bonding four fine wire thermocouples to the diode body. The unit was then encapsulated in a thermally conductive silicone adhesive.

Final testing and calibration of this controller was done extensively under different ambient temperatures up to 60°C (140°F) with a laboratory water bath accurate to $\pm 0.1^\circ\text{C}$. The final accuracy of the temperature controller for each channel is about $\pm 0.5^\circ\text{C}$. The overall accuracy from thermocouple probe to chart recorder is about $\pm 1^\circ\text{C}$.

Chart Recorder

A two channel chart recorder is used to record test pipe inlet and exit temperatures. A simple voltage divider circuit was constructed so the input of the recorder would accept the controller output signals.

Solar Energy and Weather Measurements

Incident solar radiation is measured and recorded every 15 sec by use of a pyranometer mounted on the test collector body. An Eppley brand hemispherical black and white pyranometer (type 8-48) is used for this application. It measures the sum of diffuse and direct beam radiation. The signal from the pyranometer is fed into a point plotting chart recorder. A simple voltage divider is used to match the input voltage range to the chart scale. The absolute accuracy of the pyranometer is about $\pm 3.6\%$.

Wind velocity and direction were monitored nearby the installation so that in some instances the test collector results could be related to wind convection losses.

Ambient temperature was measured continuously (with $\pm 1^{\circ}\text{C}$ accuracy) next to the collector site.

EXPERIMENTAL COLLECTOR RESULTS

Test Conditions

The test collector results were obtained under clear sky conditions with wind velocity below 1.50 m/s from the northwest or west. Also, these results were obtained with solar radiation typically between approximately 600 to 1000 W/m² and with steady flow rates (for water) within the range of 2.45-49.2 L/hr. Typical inlet temperatures of 30, 35, 40, 45, 50 and 60°C were used for the tests. The glass cover plates were cleaned as required.

Theory

Test results were calculated according to the National Bureau of Standards (NBS) proposed standards for testing solar collectors.¹ Collectors are evaluated by relating the integrated instantaneous efficiency to the ratio of net temperature change above ambient and incident solar radiation. Efficiency is defined as the ratio of useful energy collected and the solar energy intercepted by the collector. Instantaneous efficiency can be represented by the following equation:

$$\eta = \frac{Q/A}{I} \quad (1)$$

and Q/A can be represented by the following expression²

$$\frac{Q}{A} = I(\tau\alpha)_e - U_L(\bar{T}_p - T_a) \quad (2)$$

where

Q = useful energy collected (W);

A = cross sectional area intercepted (m^2);

I = solar radiation per unit time per unit area (W/m^2);

$(ta)_e$ = the effective transmission absorption factor for the collector;

U_L = the heat transfer loss coefficient for the entire collector
(W/m^2OC);

\bar{T}_p = average absorber temperature ($^{\circ}C$);

T_a = ambient temperature ($^{\circ}C$).

It is convenient to use a constant parameter (F') to compensate for the use of the average fluid temperature (\bar{T}_f) instead of the temperature (\bar{T}_p). The constant F' is usually close to unity. In terms of \bar{T}_f , Eq. (3.11) may be represented by the following:

$$\frac{Q}{A} = F' [I(ta)_e - U_L(\bar{T}_f - T_a)] \quad (3)$$

and

$$\bar{T}_f = (T_{fi} + T_{fe})/2$$

and

T_{fi} = inlet fluid temperature ($^{\circ}C$);

T_{fe} = exit fluid temperature ($^{\circ}C$).

Fitting Eq. (3) into Eq. (1) the following is obtained:

$$\eta = \left(F' (ta)_e \right) - \left(\frac{F' U_L (\bar{T}_f - T_a)}{I} \right) \quad (4)$$

and

$$T = (\bar{T}_f - T_a)$$

Equation (4) indicates that if efficiency is plotted with respect to $\Delta T/I$ a straight line will result, where the slope will be $F'U_L$ and y-intercept equal to $F'(ta)_e$.

In reality the loss coefficient, U_L and the effective transmission absorption product $(ta)_e$ are not constant and are both functions of collector temperature and ambient weather conditions. Also, $(ta)_e$ is a function of incident angle with respect to the collector. As a result, curves generated in such a manner will be somewhat general but comparable if fairly constant conditions exist. To separate these dependencies in terms of true functions an extremely accurate collector would have to be built. NBS quotes that the best collector accuracy is no better than $\pm 5\%$.

To determine the solar collector efficiency factor (F') the effective transmittance absorption product $(ta)_e$ must be calculated. This product is defined by the following expression:³

$$(ta)_e = (ta)_p + (1-t_a) \sum_{k=1}^n a_k t^{k-1} \quad (5)$$

where $(ta)_p$ = the collector cover transmittance absorption product, at some angle (p) with respect to the collector surface normal;

t_a = the cover transmittance due to absorption;

t_r = the cover transmittance due the reflection;

t = the product $(t_r) \times (t_a)$;

a_k = the ratio of the overall loss coefficient to the loss coefficient from the k-th cover to the surroundings.

For a two cover test collector, equation (5) reduces to the following equation:

$$(ta)_e = (ta)_p + (1-t_a) (a_1+a_2t) . \quad (6)$$

where t is the average solar transmittance of a single cover ($t = 0.92$).

The constants (a_1 and a_2) depend mainly upon emittance of the absorber and slightly upon ambient weather conditions and absorber temperature.

For an absorber surface with known average infrared emittance (e_i), (emittance is defined in the following section), the constants (a_1 and a_2) can be approximated. Also, ambient weather conditions must be specified. For 5 m/sec. wind at 100°C absorber temperature the following constants have been evaluated:

$a_1 = 0.15$, $a_2 = 0.62$ for $e_i = 0.95$ (non-selective absorber)

$a_1 = 0.09$, $a_2 = 0.40$ for $e_i = 0.10$ (selective absorber)

The transmittance absorption product $(ta)_o$ for near normal incidence (to the collector surface) is given by equation (7)

$$(ta)_o = \frac{a_i t_o}{1 - (1-a_o) d_o} \quad (7)$$

where

t_o = near normal total transmittance of two glass covers; ($t_o = 0.84$)

a_i = near normal average absorptance of collector absorber;

d_o = diffuse near normal reflectance (for a two cover system

$d_o=0.15$).

so for two covers equation (7) becomes:

$$(ta)_o = \frac{0.84 a_i}{0.85 + 0.15 a_i} \quad (8)$$

The transmittance due to absorption (t_a) is defined for near incident angles by the following expression:

$$t_a = \exp(-nkl) \quad (9)$$

where

k = the extinction coefficient for the cover material, for low

iron glass $k = 0.04/\text{cm}$;

l = effective thickness of material ($l = 0.24 \text{ cm}$) ;

n = number of cover plates ($n = 2$) .

evaluating equation (9) ,

$$t_a = 0.98.$$

Also, t_a could be derived from t_r or t given the average index of refraction (in the solar spectrum) for glass. This method agrees with the above result. Now, with a value for t_a , equation (6) may be equated in terms of the average absorber absorptance (a_i). Values for (a_i) will be determined by reflectance measurements presented in Section IV.

For a selective absorber (at near incident angles) equation (6) becomes:

$$(ta)_e = \frac{0.84 a_i}{0.85 + 0.15 a_i} + 0.0086 \quad (10)$$

And for a non-selective absorber it becomes:

$$(ta)_e = \frac{0.84a_i}{0.85 + 0.15a_i} + 0.015 \quad (11)$$

The correction for $(ta)_o$ in both cases is minor, with the selective absorber requiring the least correction. So, similar values for $(ta)_e$ would be obtained with slight variations from actual absorber emittance values, absorber temperature and wind velocity.

In a following section a model is presented for the collector; it also includes various parameters of the foregoing theory.

Calculation of Collector Efficiency

Another equivalent expression for instantaneous efficiency which is used for experimental data (a NBS proposed standard) is the following equation:

$$\eta = \frac{\left(\dot{m} C_p \int_{S_1}^{S_2} (T_{fe} - T_{fi}) ds \right) / A_a}{\int_{S_1}^{S_2} I ds} \quad (12)$$

where S_1 and S_2 represent limits of a time interval such as 0, 15-30 minutes;

A_a = the frontal area, receiving or aperture area (m^2);

C_p = the heat capacity of the fluid ($J/kg \text{ } ^\circ C$);

\dot{m} = the mass flow rate (kg/sec).

The quantities for heat capacity (C_p) and mass flow rate (\dot{m}) have been omitted from the integration in the numerator since they remain essentially constant.

All test pipes were evaluated by equation (12) - using six minute intervals for integration over thirty minute periods. Due to the nature of the collector, the difference in inlet and outlet temperatures were fairly constant over these thirty minute periods. The solar insolation values varied slightly in a linear manner over the interval, either decreasing or increasing except for solar noon. In most cases, the overall insolation characteristics exhibited a classical Gaussian distribution.

The types of surfaces tested were three selective absorbers of the Chromonyx black chrome type and one non-selective absorber of a commercial black spray paint. The non-selective absorber is made by Cal Custom/Hawk Company and it contains 4.8% black iron oxide in a modified silicone resin and stable to 649°C.⁴

The designations and specifications of the absorbers are as follows:

R1 - 1.0 micron of black chrome on 12.7 microns of nickel on cold rolled mild steel.

R16 - 1.0 micron of black chrome on mild steel.

R9 - 1.0 micron of black chrome on copper.

HP1 - a thick coating (several hundred microns) of heat proof black paint on galvanized steel.

Galvanized steel was used on the HP1 pipe due to its corrosion resistance. The oxidation of steel interferes with adherence of the paint film.

In Figures 8a-8d are shown the test collector results for the aforementioned samples. All lines are curve fit by a linear regression least squares approximation to represent the relationships of each of the curves; they are plotted in Fig. 9.

The equations, slopes and intercepts are shown in Table 1.

To determine the actual collector performance factor (F') the value of $(ta)_e$ has to be determined. The product $(ta)_e$ will be determined in the following section along with the optical properties of various coatings.

The plating conditions for R1, R4 and R16 are as follows:

1. Cleaning by an electrolytic alkaline kelating cleaner, 88°C at 76-86 mA/cm².
- *2. Nickelplate (dull finish, NuSat process).
3. Black chrome (Chromonyx) plate, 216 mA/cm², 24°C for 2-3** minutes at 24 volts.
4. Water rinse, alcohol rinse and dry.

*Only for Sample R1. **Depends on thickness desired.

Discussion of Results

In some cases the scatter in the data points is representative of a situation one might expect for experimental conditions which would vary slightly with time. A true but very difficult procedure would be to control all collector parameters, except for insolation and resultant temperature differences, in such a way so they are time invariant. This might be achieved by the use of a completely simulated (fixed environment) collector.

An overall view of the data reveals that for the selective black chrome surface the data points for efficiency are mainly between 50-70%. These values indicate, under near optimal conditions, the efficiency at which the collector usually operates. The non-selective paint has 40-60% efficiency under the same conditions. The efficiency on the y-intercept is not a realistic operating point because the collector is at the ambient temperature ($\bar{T} = T_a$ or $\Delta T=0$). Frequently, this intercept value is mistakenly reported as optimum efficiency.

In reality, the curve fit for the data points is not linear except in the central region. Near the region of the y-intercept the curve should flatten out and in the region of the x-intercept the curve should dip downward. These effects occur because the loss coefficient (U_L) is a function of temperature. At higher temperatures the loss coefficient increases and at lower temperatures it decreases. The slope ratio between black paint and black chrome is approximately 2, which indicates that black paint will not perform as efficiently as black chrome at a given temperature. Also, the difference in x-axis intercept shows that black chrome will function at higher temperatures than black paint.

The black chrome plated copper pipe exhibits the highest net efficiency. This effect is due partially to the difference in thermal conductivity between copper and steel. Of the pipes tested, the copper pipe has approximately 2.5 the thermal conductance of the steel pipe. Choosing copper rather than steel for pipe material would depend upon the relative cost of materials and collector fluid flow rates (absorber heat transfer rate).

The effect of nickel plating steel creates only a slight rise in both the loss coefficient and efficiency of the absorber (see Fig. 9). Although the efficiency to use black chrome directly on steel for collectors operating below 100°C.

CALCULATION OF REFLECTANCE PARAMETERS

By integration of $(1-r_w)$ where r_w is near-normal hemispherical spectral reflectance, over the solar spectrum the integrated absorptance (a_i) is obtained. Also, by integration of $(1-r_w)$ over the 100°C blackbody spectrum the integrated emittance (e_i) is obtained. The higher the ratio of these values (a_i/e_i) the greater the selectivity. Spectral reflectance measurements are shown in figures 10a, b.

The integrated results are shown in Table 2 for 20°C measurements. From these results one can calculate (by using equations 10 and 11) the effective transmission absorption product $(ta)_e$ for the test collector. Also, the collector performance coefficient (F') and the loss coefficient (U_L) may be obtained. These results are summarized in Table 3.

HEAT TRANSFER MODEL FOR THE SOLAR TEST COLLECTOR

When analyzing a collector's performance and thermal loss characteristics, it is important to model the collector. A model such as the one to follow can be very helpful in evaluating a particular collector characteristic. The following development is a modified Duffie & Beckman model (ref. 3). Two versions of the same model will be presented, first a complete model depicted in Fig. 11a and finally a simplified version shown in Fig. 11b.

A. Rigorous Model

The various components of Fig. 11a are listed as follows:

I = total incident radiation (direct and diffuse components)
converted into the plane of the collector, W/m^2 .

r = reflection loss of collector cover, the loss is about 8%
per glass plate.

R_n = thermal resistance elements in $m^2 \text{ } ^\circ C/W$ where
 $n = 1, 2, 3, 4, 5$.

Q = heat available for the heating of fluid.

T_x = temperature at locality x , $^\circ C$.

The modeling of the resistive components can be expressed as:

$R_1 = 0$ for low temperature collectors and for the test collector.

$R_2 = L/K$ where

L = thickness of insulation, $L=0.19m$;

K = thermal conductivity of insulation $K=0.017 \text{ W/m}^\circ C$.

$R_2 = 11.2 \text{ } ^\circ C m^2/W$.

$R_6 = 0$, edge loss effect (in small collectors, this can be a

significant term). In this case, it may be neglected due to strip heater simulation of large collector.

$R_3 = (h_{p-c2} + h_{r2})^{-1}$ pipe to cover heat transfer where

h_{p-c} = convective heat transfer coefficient pipe to cover 2;

h_{r2} = radiative heat transfer coefficient pipe to cover 2.

$R_4 = (h_{c2-c1} + h_{r2})^{-1}$ cover to cover heat transfer where

h_{c2-c1} = convective heat transfer coefficient cover 2 to cover 1;

h_{r1} = radiative heat transfer coefficient cover 2 to cover 1.

$R_5 = (h_w + h_{r4})^{-1}$ cover to ambient heat transfer where

h_w = wind convection coefficient;

h_{r4} = radiative heat transfer coefficient cover 1 to sky.

Now to evaluate the heat transfer coefficients:

For radiative heat transfer:

$$h_{r2} = \frac{\sigma(T_p - T_{c2})(T_p^2 + T_{c2}^2)}{\left(\frac{1}{e_p} + \frac{1}{e_{c2}} - 1\right)} \quad (13)$$

$$h_{r1} = \frac{\sigma(T_{c2} - T_{c1})(T_{c2}^2 + T_{c1}^2)}{\left(\frac{1}{e_{c1}} + \frac{1}{e_{c2}} - 1\right)} \quad (14)$$

$$h_{r4} = e_{c1} \sigma (T_{c1}^2 + T_s^2) (T_{c1} + T_s) \left(\frac{T_{c1} - T_s}{T_{c1} - T_a} \right) \quad (15)$$

where (σ) Stephan-Boltzmann constant

$$\sigma = 5.669 \times 10^{-8} \text{ watts m}^{-2} \text{ } ^\circ\text{K}^{-4}$$

e_x = Total emittance (often called the emissivity) of element

x; e_x is a function of temperature.

T_x = Temperature of element x (p=pipe, c=cover, a=ambient, s=sky)

For convective heat transfer

$$h_{p-c2} = \frac{N K_a}{L_{p-c2}} \quad (16)$$

$$h_{c2-c1} = \frac{N K_a}{L_{c2-c1}} \quad (17)$$

where

N = Nusselt number (pure condition resistance/pure convection resistance)

L_{x-x1} = spacing between element x and x_1 , $L_{p-c2} = 0.0254m$,

$L_{c2-c1} = 0.019m$

a = thermal conductivity of air, 0.026 W/m°C, 20°C

Using Tabor's approximation for a 45° tilt

$$h_{p-c2} = \left(\frac{1.14 (T_p - T_{c2})^{0.310}}{L_{p-c2}} \right) (1 - 0.0018 (\bar{T} - 10)) \quad (18)$$

$$h_{c2-c1} = \left(\frac{1.14 (T_{c2} - T_{c1})^{0.310}}{L_{c2-c1}} \right) (1 - 0.0018 (\bar{T} - 10)) \quad (19)$$

where

\bar{T} = the average air temperature between the two elements in question.

The wind convection coefficient can be expressed as

$$h_w = 5.7 + 3.8V \quad (20)$$

where

V = velocity of air in M/sec..

Now the total collector loss coefficient (U_L) can be evaluated in terms of the temperatures T_s , T_p , T_a , T_{c1} , T_{c2} and by emittances e_{c1} , e_{c2} , e_p where

$$U_L = \left[\sum_{1}^6 R_1 \right]^{-1} \quad (21)$$

which reduces to the following, for this collector:

$$U_L = \left[\sum_{2}^5 R_1 \right]^{-1} \quad (22)$$

B. Simplified Model

For an approximation, the model can be simplified as shown in Fig. 11b.

Where the parameters noted in this figure are as follows:

S = energy actually reaching the collector pipes;

U_t = top loss coefficient;

U_b = bottom loss coefficient = $\frac{1}{R_2}$

$U_b = K/L = 0.0893 \text{ W/}^\circ\text{Cm}^2$;

$$U_t = \frac{1}{R_3 + R_4 + R_5} = \left(\frac{1}{h_{p-c2} + h_{r2}} + \frac{1}{h_{c2-cl} + h_{r1}} + \frac{1}{h_w + h_{r4}} \right)^{-1} \quad (23)$$

U_t is estimated after Klein⁵ modified for two covers at 45° tilt angle.

$$U_t = \left(\frac{2}{(344/T_p) [(T_p - T_a)/(2+f)]^{0.31}} + \frac{1}{5.7 + 3.8V} \right)^{-1} \quad (24)$$

$$+ \left(\frac{\sigma(T_p + T_a)(T_p^2 + T_a^2)}{(0.085 + 0.915 e_p)^{-1} + [(3+f-2e_g)/e_g]} \right) \quad (25)$$

for two cover plates:

$$f = (1.116 - 0.04464h_w + 5.58 \times 10^{-4}h_w^2) \quad (26)$$

where h_w is defined by (20).

The experimental loss coefficient (U_L exp.), for samples R1, R4, R16 and HPl, can be compared to a calculated U_t using spectral reflectance data. Solving equations (20), (25) for $V = 1.5$ M/sec. then $h_w = 11.4$, $f = 0.680$.

Now solving for U_L where $U_L = U_t + U_b$, $e_g = .88$, and $T_p = 100^\circ\text{C}$. Emittance values for 100°C have been estimated from empirical data by curve fitting. These values and results are shown in Table 4.

The experimental values compared to the model show fair agreement. These values differ mainly due to the design difference between a flat plate collector and the test collector. So modeling the test collector as a flat plate collector appears to be a poor assumption.

CONCLUSIONS AND RECOMMENDATIONS

A solar test collector has been designed and constructed which was used to measure the efficiency of four collector surfaces--three selective black chrome and one non-selective black paint. This collector was compensated for edge losses and measures differential pipe temperatures with 1°C accuracy. The absolute uncertainty of the collector measurements of efficiency are about 10% (for example a value of 60% efficiency could vary from 54-66%), while it has a few percent uncertainty in reproducibility and is limited by the accuracy of the mass flow rate measurement. The collector typically operates at low flow rates (0-49 L/hr) up to temperatures of 100°C at atmospheric pressure. The collector is designed so collector pipes may be removed with ease and it has the ability to regulate the fluid inlet temperatures within 1°C accuracy. The inlet temperatures are adjustable ($25-90^{\circ}\text{C}$) and are maintained by an electronic controller. The collector includes a manual tilting stand for orientation to the sun. A heat transfer model has been presented which models this collector's performance. Calculated and experimental values are in fair agreement.

The four surfaces tested (R1, R9, R16 and HP1) are representative of a range of possible combinations. The loss coefficients for these four surfaces show that black paint has about a factor of two times greater loss than for the black chrome samples. The loss coefficient for the black chrome samples was about the same-- $3.8 \text{ W/m}^2 \text{ }^{\circ}\text{C}$ for all three. Black chrome on copper was the most efficient of the surfaces tested; probably, this is due to reflectance and high thermal conductivity of copper. Black chrome on nickel-plated steel and steel substrates

had comparable properties. The effect of nickel plating steel accounted for only a 0.04 rise in efficiency for the absorber. Nickel plating may not be cost effective in light of this result. For the low flow rates at which collector operated, the effect of the high thermal conductivity of copper is not a greater as it could be in promoting high heat transfer rates. If a factor of 2-6% efficiency for black chrome (at $\Delta t=0$) are 0.77 for the copper sample, 0.75 for nickel plated steel, 0.71 for steel and at least 0.05-0.10 lower than the intercept values.

Spectral reflectance measurements are used to obtain optical parameters such as solar absorptance and infrared emittance. The best solar selectivity characteristics were exhibited by 1.0 micron of black chrome on copper ($a_i/e_i = 18.5$). Almost all combinations showed good selectivity. The effect of the nickel layer was marginal in promoting higher selectivity for the steel samples and it degraded selectivity on the copper samples.

ACKNOWLEDGMENTS

I am particularly grateful to Professor Jack Washburn for his guidance and support throughout this project. I wish to thank my colleague and friend, Dr. Lawrence Crooks, for his invaluable help with the design and construction of the electronic controller. I am thankful to Mr. George Cunningham of Lockheed for his advice and use of spectral reflectance equipment.

This work was performed under the auspices of the U.S. Energy Research and Development Administration.

REFERENCES

1. NBS-National Bureau of Standards, U.S. Dept. of Commerce, Development of Proposed Standards for Testing Solar Collectors and Thermal Storage Devices, Technical Note, 899, p. 27, 1976.
2. R. W. Bliss, Solar Energy, 3-4, 55(1959), (NBS states other investigators also use this technique).
3. J. A. Duffie and W. A. Beckman, Solar Energy Thermal Processes Wiley, New York, 1974.
4. C. S. Moore, T. S. Ashley III, et al., Analytical and Experimental Treatment of a Spray on Selective Coating Applied to Collector Design, Proceedings North American Solar Energy Society, Conference, Winnipeg, Manitoba, Canada, Vol. 6, August, 1976, p. 187.
5. S. A. Klein, M. S. Thesis, "The Effects of Thermal Capacitance Upon the Performance of Flat-Rate Solar Collectors" University of Wisconsin, 1973.

Table 1. Collection efficiency parameters of Figs. 8 and 9.

Type	Figure Number	Equation	Correlation Coefficient
R1	8a	$\eta = -3.6x + 0.75$	$r^2 = 0.992$
R16	8b	$\eta = -3.3x + 0.71$	$r^2 = 0.973$
R9	8c	$\eta = -3.5x + 0.77$	$r^2 = 0.979$
HP1	8d	$\eta = -6.8x + 0.66$	$r^2 = 0.971$

Type	Slope ($-F'U_L$) (W/°Cm ²)	y Intercept ($F'(ta)_e$)	x intercept (°Cm ² /W)
R1	-3.6	0.75	0.208
R16	-3.3	0.71	0.214
R9	-3.5	0.77	0.222
HP1	-6.8	0.66	0.097

Table 2. Integrated reflectance parameters.

	R1	R9	R16	HP1
a_i	0.958	0.942	0.92	0.95
e_i	0.070	0.051	0.070	0.832
a_i/e_i	13.7	18.5	13.1	1.14

Table 3. Collector performance and loss coefficients.

	R1	R16	R9	HP1
$(\tau\alpha)_e$	0.818	0.791	0.807	0.819
F'	0.916	0.898	0.954	0.806
U_L	3.9	3.8	3.7	8.4 (W/°Cm ²)

Table 4. Comparison between experimental and modeled loss coefficients.

	R1	R16	R9	HP1
e_i (est) 100°C	0.07	0.07	0.10	0.83
U_L (exp)	3.93	3.68	3.67	8.44 (W/°Cm ²)
U_L (cal) 100°C)	2.24	2.24	2.14	3.65 (W/°Cm ²)

FIGURE CAPTIONS

- Fig. 1. Solar test collector flow chart.
- Fig. 2. Solar test collector in operation, side view.
- Fig. 3. Solar test collector in operation, rear view.
- Fig. 4. Test collector body, cross section view.
- Fig. 5. Test collector body, top view with cover removed.
- Fig. 6. Temperature measuring and pipe sealing technique shown in cross section.
- Fig. 7. Electronic control design showing how string heaters and waterbath temperature are controlled automatically.
- Fig. 8. Efficiency versus ratio of average temperature above ambient and solar radiation.
- a) Black chrome on nickel plated steel (R1).
 - b) Black chrome on Steel (R16).
 - c) Black chrome on Copper (R9).
 - d) Black paint on galvanized steel (HP1).
- Fig. 9. Comparative efficiency plots for absorber surfaces in Fig. 8. F' and U_L are respectively the collector performance and loss coefficients.
- Fig. 10. Hemispherical near-normal spectral reflectance for absorbers.
- Fig. 11. Schematic collector model in terms of thermal resistance
- a) Rigorous model and b) Simplified model.

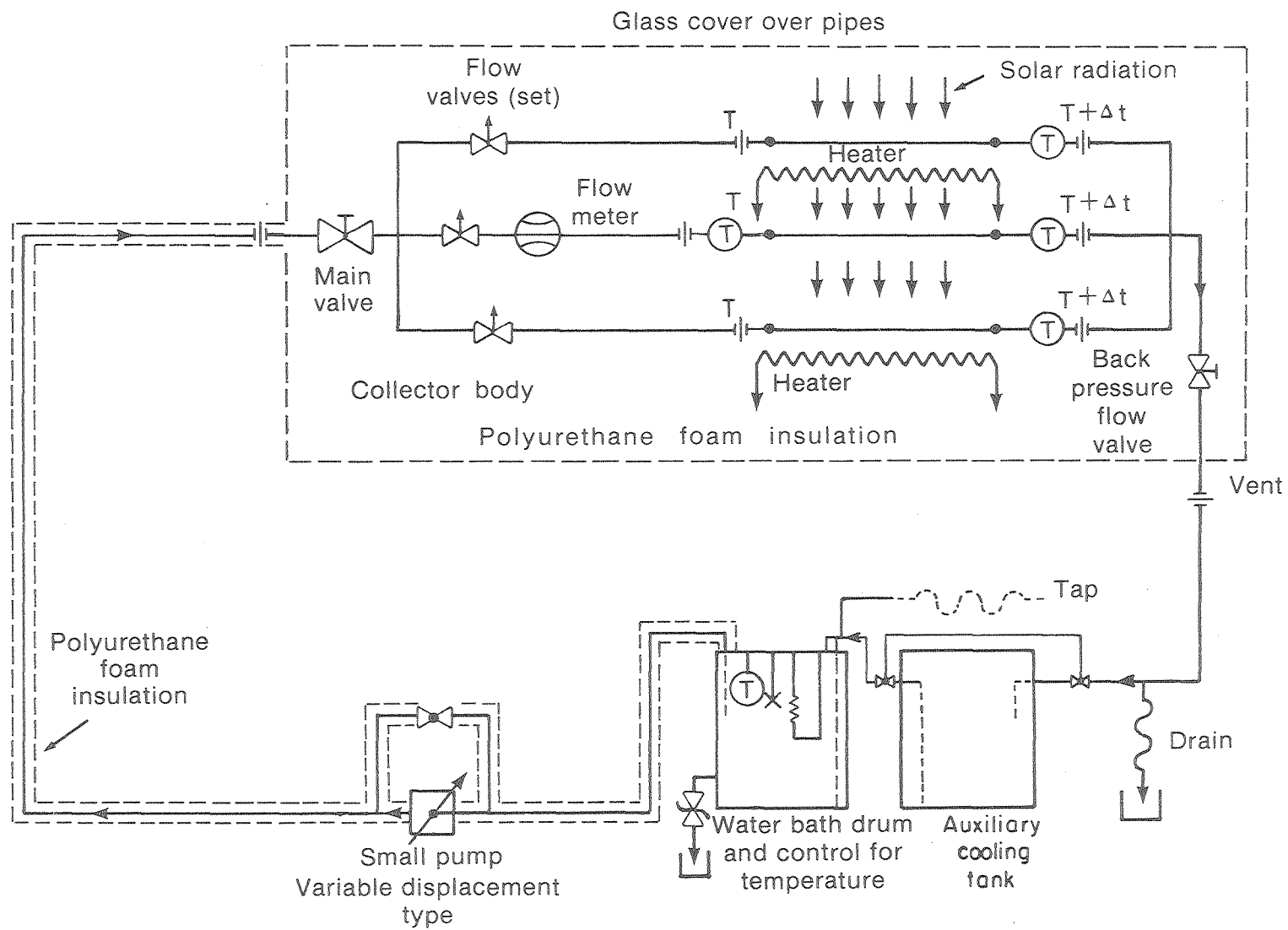
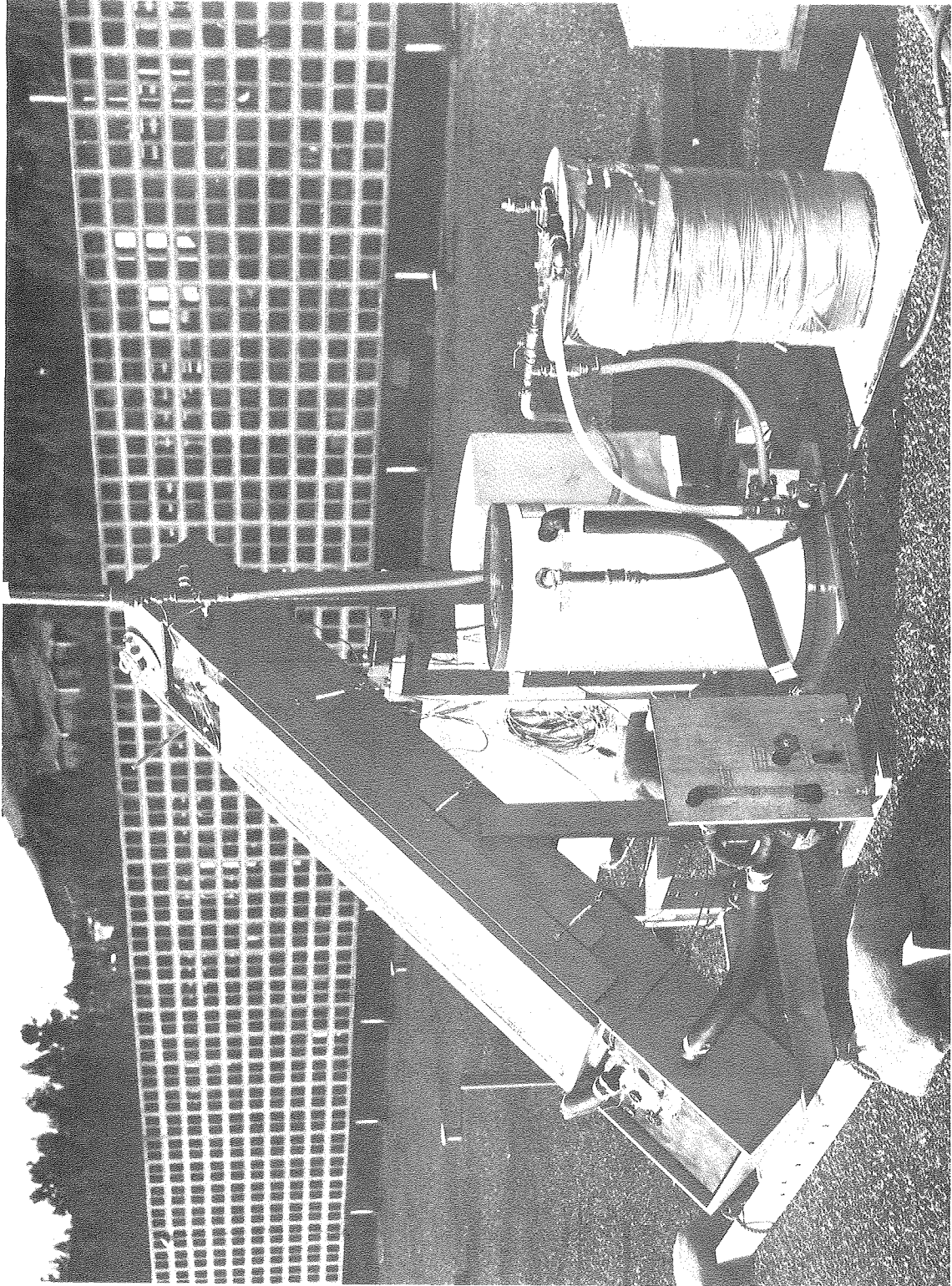


Fig. 1

XBL-7611-4465A



CEB 770-9662

Fig. 2

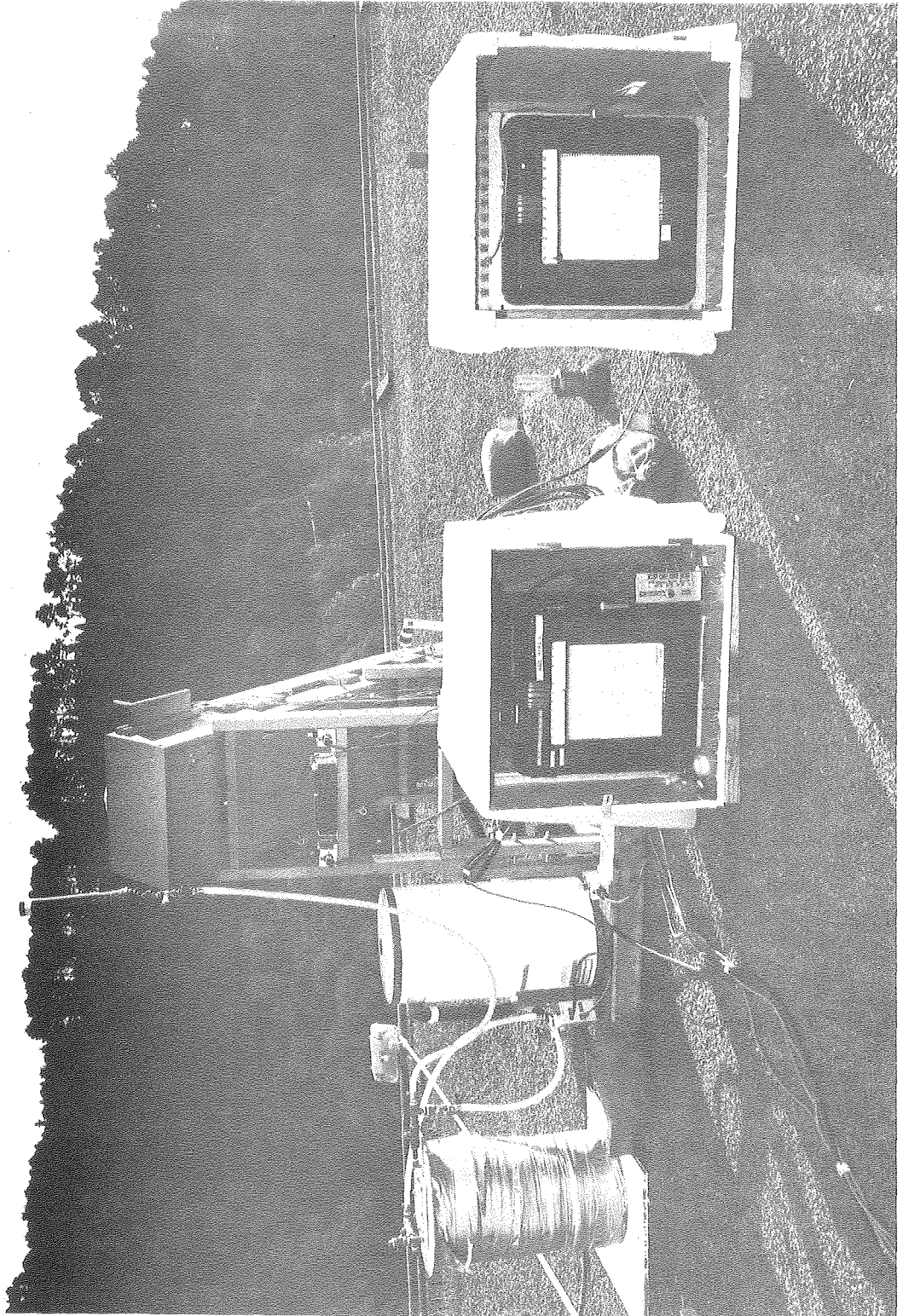
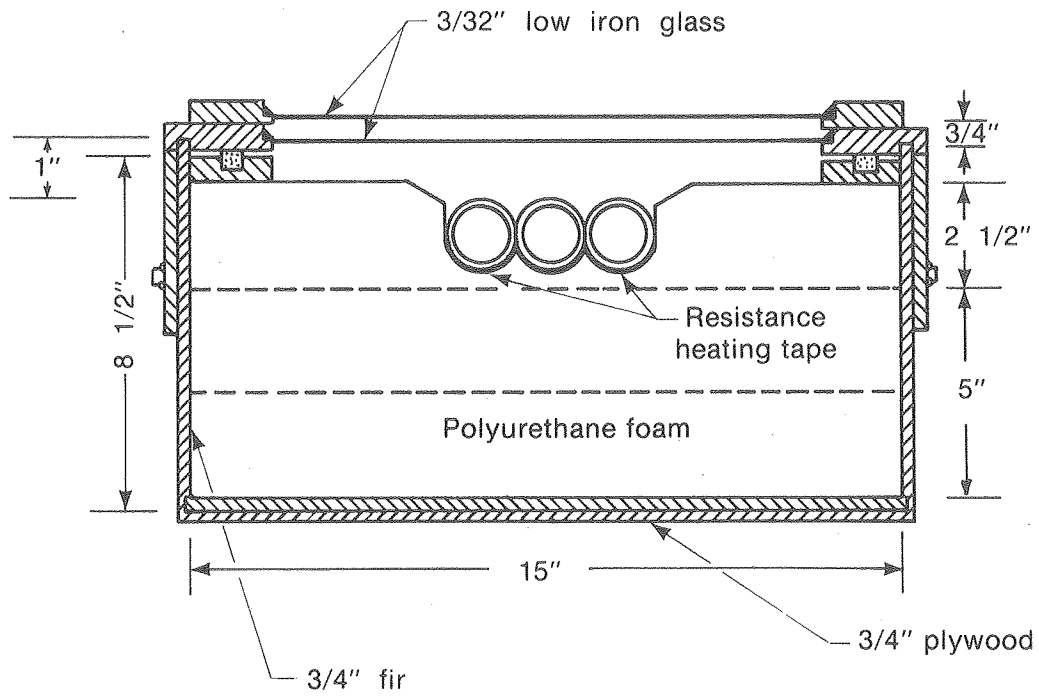


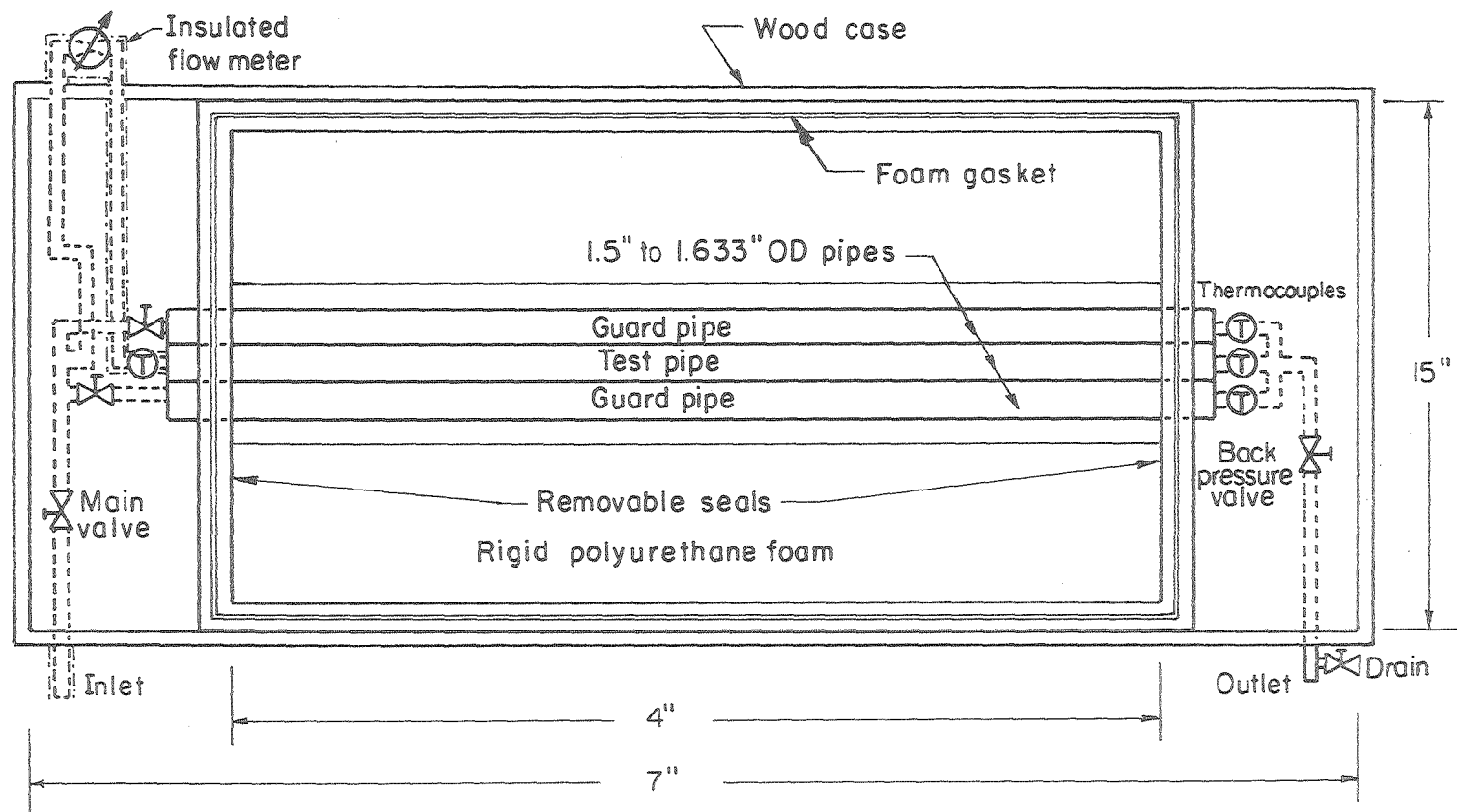
Fig. 3.

CBB 770-9664



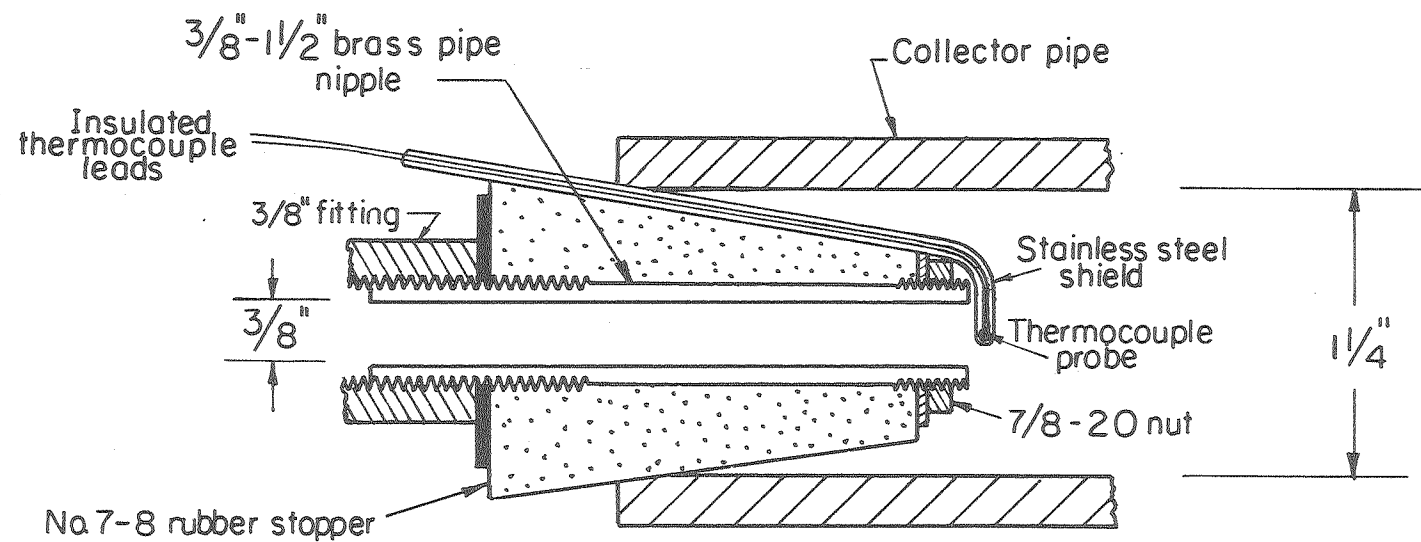
XBL-7611-4466

Fig. 4.



XBL 78I-4486

Fig. 5.



XBL 7611-4469A

Fig. 6.

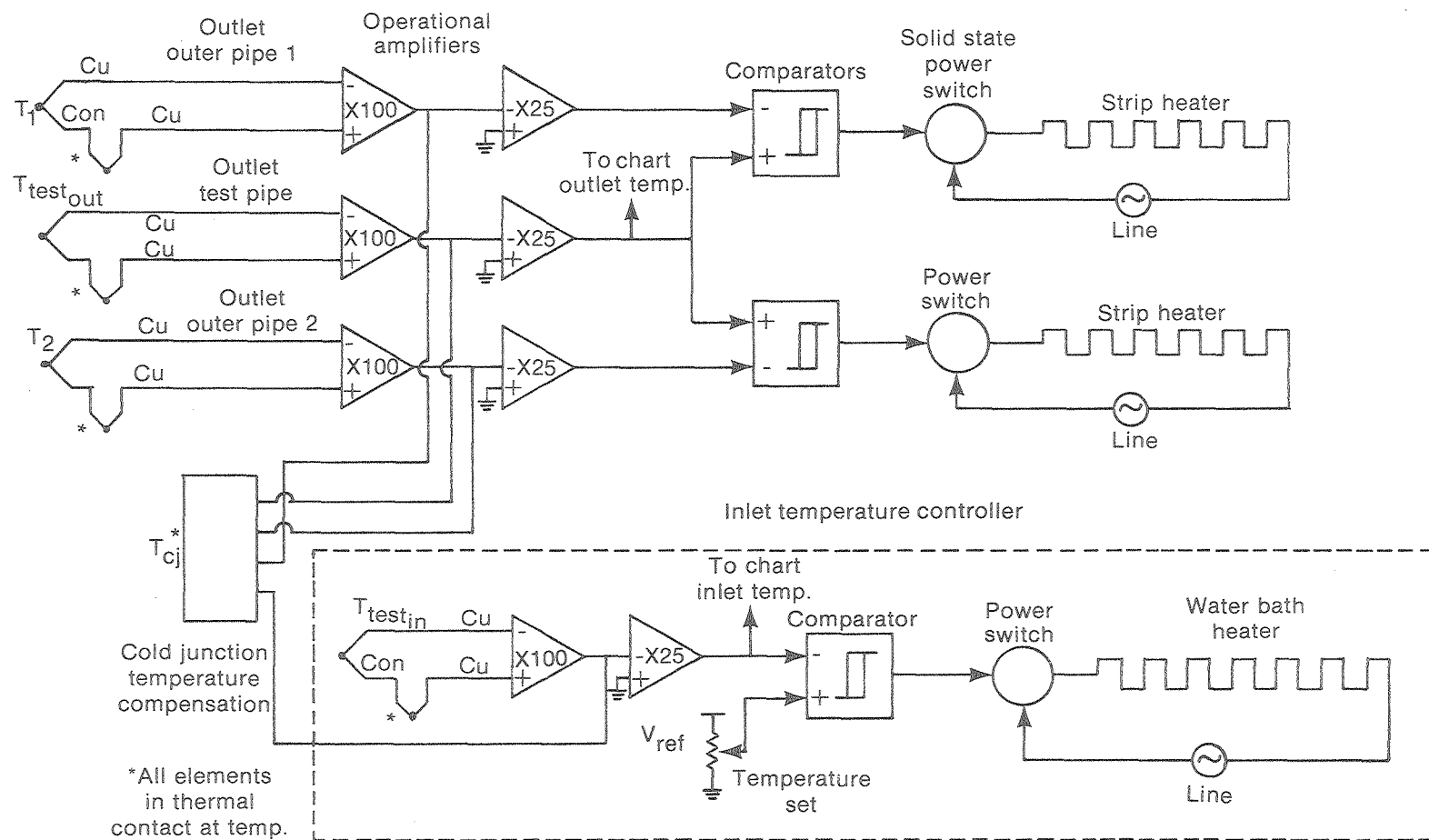


Fig. 7.

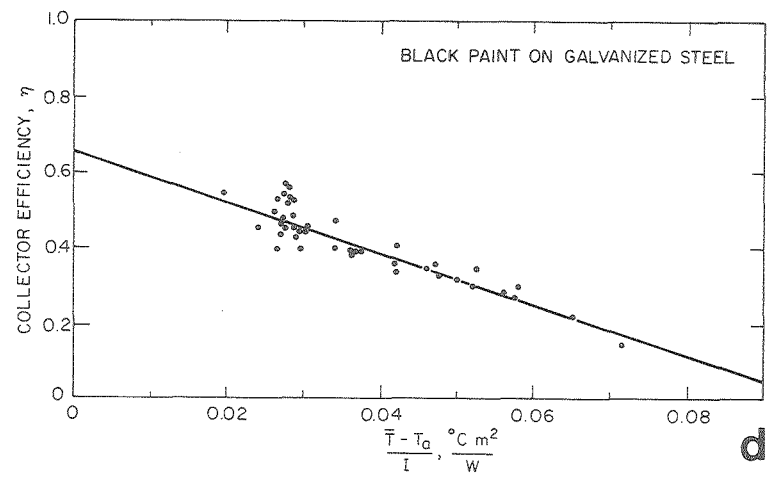
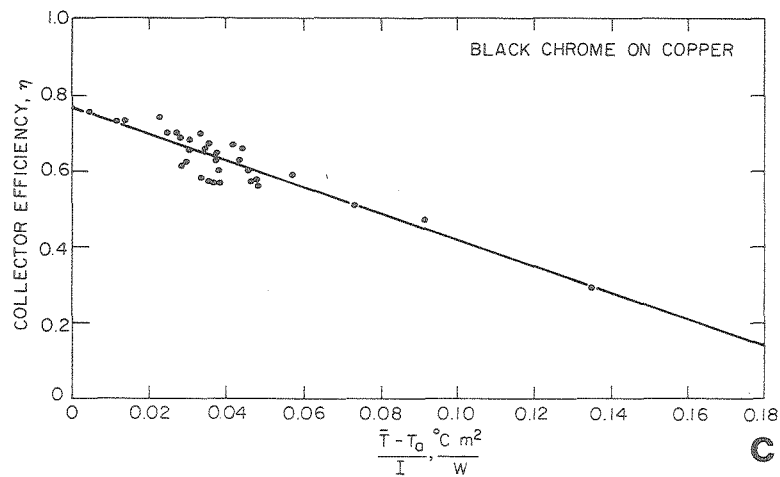
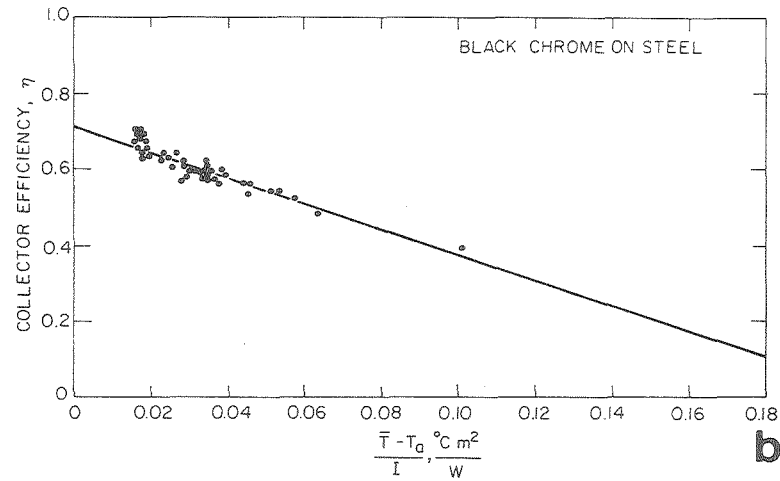
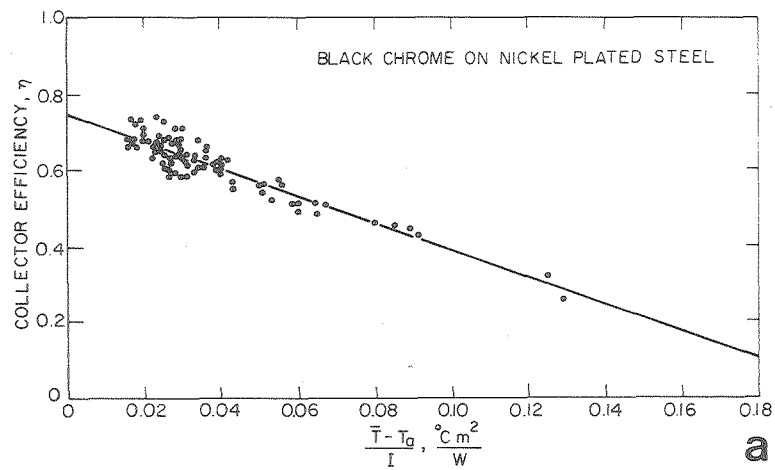
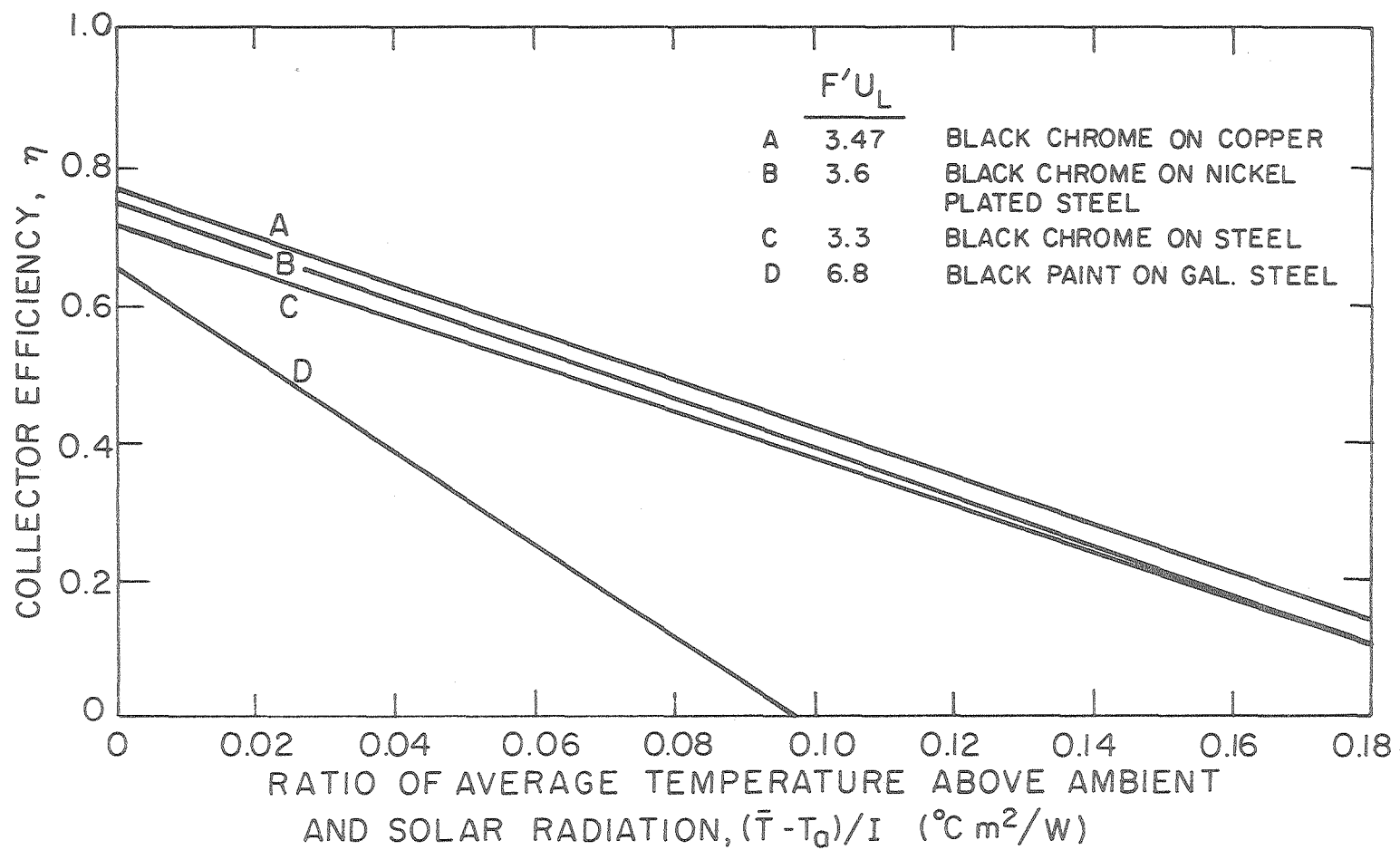


Fig. 8.

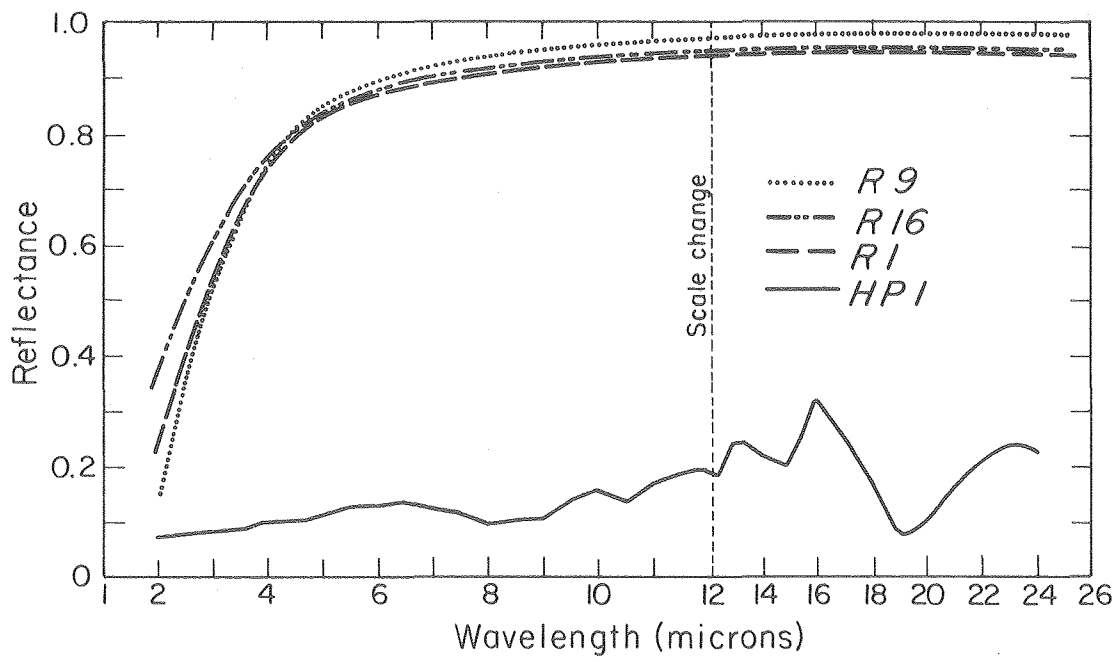
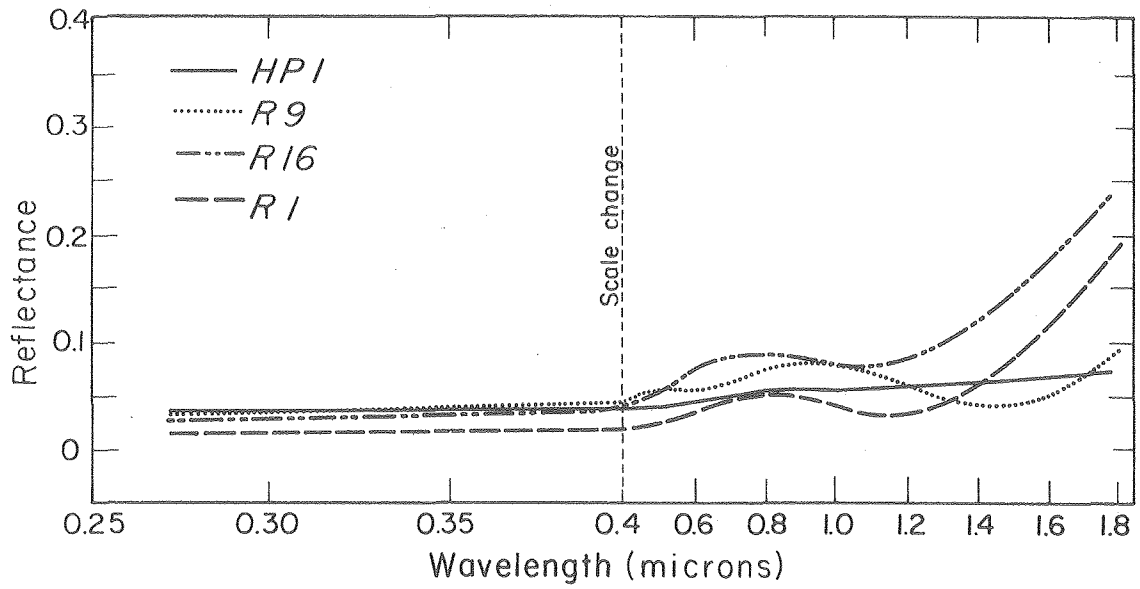
XBL 774-5329A



-43-

XBL774-5328A

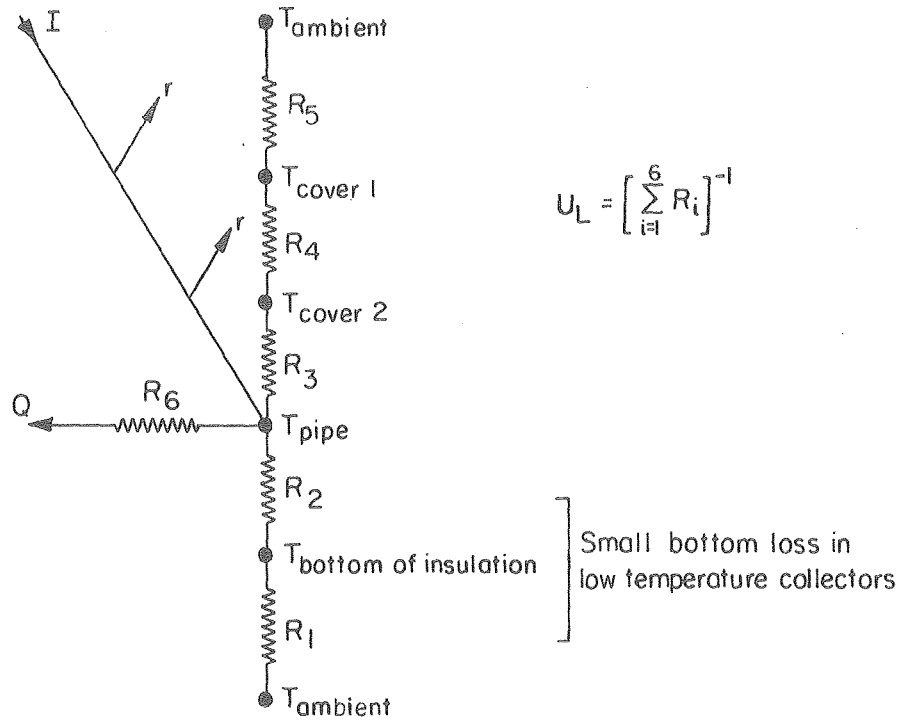
Fig. 9.



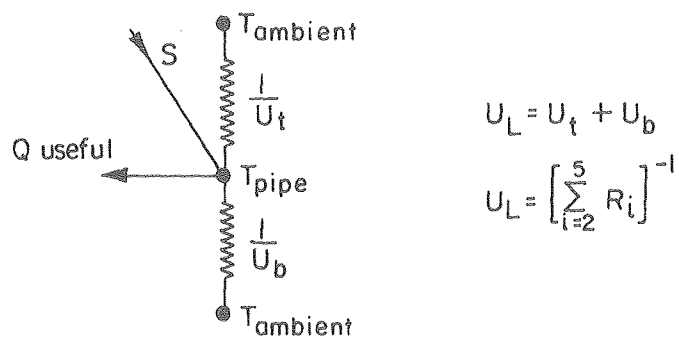
XBL 7710-6201A

Fig. 10.

A. Rigorous Model



B. Simplified Model



XBL 781-4419A

Fig. 11.

This report was done with support from the United States Energy Research and Development Administration. Any conclusions or opinions expressed in this report represent solely those of the author(s) and not necessarily those of The Regents of the University of California, the Lawrence Berkeley Laboratory or the United States Energy Research and Development Administration.